Emerging hot Spot Analysis and the Spatial-temporal Trends of NDVI in the Jing River Basin of China

Bin Xu (xubin@chd.edu.cn)
Changan University: Chang'an University https://orcid.org/0000-0002-6367-5377
Bin Qi
Chang'an University
Kai Ji
Chang'an University
Zhao Liu
Chang'an University
Lin Deng
Chang'an University
Ling Jiang
Chang'an University

Research Article

Keywords: Emerging hot spot analysis, Jing River Basin, NDVI, Trends

Posted Date: May 28th, 2021

DOI: https://doi.org/10.21203/rs.3.rs-482991/v1

Version of Record: A version of this preprint was published at Environmental Earth Sciences on January 1st, 2022. See the published version at https://doi.org/10.1007/s12665-022-10175-5.

Emerging hot spot analysis and the spatial-temporal trends of NDVI in the Jing River Basin of China

Bin Xu [a,b,c,d,*], Bin Qi[a], Kai Ji[a], Zhao Liu[a], Lin Deng[a], Ling Jiang[a]

[a]*School of Water and Environment, Chang'an University, No. 126 Yanta Road, Xi'an, 710054, Shaanxi, China;*

[b]*Key Laboratory of Degraded and Unused Land Consolidation Engineering, Ministry of Natural Resources, No. 7 Guangtai Road, Xi'an, 710075, Shaanxi, China;*

[c]*Key Laboratory of Subsurface Hydrology and Ecological Effects in Arid Region, Ministry of Education, Chang'an University, No. 126 Yanta Road, Xi'an, 710054, Shaanxi, China*

[d]*Shaanxi Key Laboratory of Land Consolidation, No. 126 Yanta Road, Xi'an, 710054, Shaanxi, China;*

*Corresponding author.

E-mail addresses: xubin@chd.edu.cn (Bin Xu)

Abstract: As an important indicator of vegetation coverage, the Normalized Difference Vegetation Index (NDVI) reflects the changing pattern and evolving trend of the environment. In the Loess Plateau, vegetation plays a critical role in soil and water conservation, which strongly affects the achievement of sustainable development goals. The study of the spatial distribution and temporal trends of NDVI is of great practical importance for the planning of soil and water conservation measures, the evaluation of environmental situation. In this study, the NDVI, precipitation and land cover data of the Jing River Basin were collected, the emerging hot spot and cold spot patterns of NDVI were examined, the characteristics of spatial distribution and temporal variation of the NDVI in the basin were analyzed, the impacts on NDVI changes from climate, land cover change have been discussed. The results show that the NDVI in Jing River Basin shows a spatial trend of decreasing from northwest to southeast. The emerging hot spot analysis results show that diminishing cold spot, oscillating hot spot, intensifying hot spot are predominant patterns in the basin. The whole basin shows the statistically significant upward trend of high-value aggregation of NDVI. The temporal trend of NDVI in the basin varies from-0.0171 to 0.0185 per year. The increasing trend of vegetation coverage in the basin is statistically significant. The positive correlation between the NDVI and the precipitation mainly observed upstream of the basin, revealing that the growth of vegetation in the Loess Plateau is more dependent on the water supply from the precipitation. Land cover transition patterns and the land use patterns also impact the spatial-temporal trends of the vegetation coverage in the basin. The study results may helpful for the vegetation restoration, soil and water conservation and sustainable development

of the Jing River Basin.

Keywords: Emerging hot spot analysis; Jing River Basin; NDVI; Trends;

Declarations

Funding

This research was supported by the National Natural Science Foundation of China (41971033), the Natural Science Basic Research in Shaanxi Province of China (Program No. 2019JM-512), the Key Laboratory of Degraded and Unused Land Consolidation Engineering of the Ministry of Natural Resources (SXDJ2019-13), the Fundamental Research Funds for the Central Universities (CHD300102291507), the Programme of Introducing Talents of Discipline to Universities (B08039), Fund Project of Shaanxi Key Laboratory of Land Consolidation (2019-JC01).

Conflicts of interest/Competing interests

The authors declare that they have no known competing financial interests or personal relationships that could have appeared to influence the work reported in this paper.

Availability of data and material

Not applicable

Code availability

Not applicable

Authors' contributions

Not applicable

Ethics approval

Not applicable

Consent to participate

Not applicable

Consent for publication

Not applicable

1. Introduction

Vegetation is an important part of the ecosystem and an intermediate link in the soil-plant-atmosphere continuum (Zhang and Huang 2021). It has the functions of transporting water, carbon sequestration, releasing oxygen and so on (Wang et al. 2016, Paustian 2014). Vegetation can weaken soil erosion caused by rainfall, reduce land surface runoff, alter groundwater quality, and decrease river sediment content (Aber et al. 2010, Jin et al. 2021; He et al. 2020; He and Wu 2019). Vegetation coverage is a key factor in environmental protection and land resource planning. Vegetation coverage, to a large extent, represents the state of the terrestrial environment and ecosystem. Vegetation coverage is affected by anthropological activities and climate change, directly influencing regional socio-economic development, the stability and safety of the environment and the ecosystem (Jin et al. 2021).

Remote sensing is an important technology to quickly obtain the vegetation types and vegetation coverage in a large area, and it can perform long-term dynamic monitoring of vegetation coverage at different scales. Normalized difference vegetation index (NDVI) was proposed by Kriegler et al. in 1969, is one of the most widely used vegetation indices based on remote sensing data, also known as biomass index change, which can separate vegetation from water and soil. It has been widely used in ecological and environmental monitoring, drought monitoring, vegetation growth capacity evaluation, land use, and so on (Huang et al. 2021). In recent years, many scholars have conducted more in-depth research on the temporal trend and spatial distribution of vegetation coverage based on the NDVI (Jin et al. 2021).

The Jing River locates in the Yellow River Basin and is the second largest tributary of the Yellow River (Li et al. 2013). The Jing River flows through the Loess Plateau, where soil erosion is serious (Liu et al. 2018). While recharging the Yellow River, it also brings a large amount of sediment to the Yellow River. The Jing River is also the main source of irrigation water for many large irrigation districts in the Guanzhong Plain of Shaanxi Province (Xu et al. 2019; Zhang et al. 2018a). For a long time, the problems of vegetation degradation, soil erosion, runoff reduction, and water pollution in this area have attracted much attention (Li et al. 2014), making it a landmark object for studying soil and water conservation, ecological protection, human health risk assessment, and sustainable development of the Loess Plateau and the Yellow River Basin (Zhang et al. 2020, 2021, Deng et al. 2021, Ning et al. 2016, Chang et al. 2016; Li et al. 2018, 2019a, b). A lot of research work concerning the Jing River Basin has been carried out by scholars worldwide (Li et al. 2013, Liu et al. 2018, Xu et al. 2019).

In the past two decades, through a series of environmental restoration measures such as the Grain for Green Program, the vegetation coverage in the basin has been improved, the spatial distribution of land-water resources has undergone significant changes, and soil erosion has been effectively curbed (Delang and Yuan 2015). However, problems of water shortage, water use conflicts, and ecosystem degradation in the basin still exist. In 2019, the ecological protection and high-quality development of the Yellow River Basin have become a national strategic goal in China (Li 2020a, b). Therefore, analyzing the characteristics of vegetation changes in the Jing River under the influence of climate change and anthropological activities is important for optimizing the allocation of regional land-water resources, adjusting soil and water conservation patterns, promoting ecological restoration, and achieving sustainable high-quality development goals in the Yellow River Basin.

This study was conducted for the first time using the emerging hot spot analysis method to analyze the change characteristics of NDVI in the Jing River Basin. This study aims to: (1) analyze the aggregation mode and hot spots trend of vegetation cover in the basin, (2) obtain the spatial-temporal trends of vegetation cover in the study area, and (3) discuss the relationship between vegetation and climate change, anthropological activities in the basin. This study may provide a meaningful reference for the vegetation restoration, soil and water conservation, and sustainable development of the Jing River Basin.

2. Materials and methods

2.1 Study area

Located in the middle reaches of the Yellow River, the Jing River is a secondary tributary of the Yellow River and the largest tributary of the Wei River (Fig. 1). The Jing River has a total length of 455.1 km and a drainage area of 45,400 km^2 (Li et al. 2013, Liu et al. 2018). It straddles the three provinces (regions) of Gansu, Ningxia, and Shaanxi. The basin is divided into mountainous forest areas in the southwest, mountainous river areas in the southeast, and hilly areas of the Loess Plateau in the central and northern parts (Li et al. 2013, Liu et al. 2018). The basin is a typical temperate continental climate zone, located in the transition zone from a semi-humid climate to a semi-arid climate (Li et al. 2013, Liu et al. 2018). The annual average precipitation from 1981 to 2020 is 508.59 mm, and the annual average temperature is 9.7°C. The Jing River flows through the high-intensity soil erosion area of the Loess Plateau. A large scope of the basin is covered by thick loess which has poor corrosion resistance. The soil erosion in the basin has been severe

for a long time, and the ecological environment is fragile (Li et al. 2013, Liu et al. 2018).

The Jing River Basin is across the typical agropastoral regions of Northwest China. The dominating land cover is cultivated land, grassland, and forest, with percentages of 47.0%, 32.9%, and 16.5 %, respectively. The Jing River Basin is a very important irrigation water source for large irrigation districts. The proportion of agricultural water consumption exceeds 60% of the total water resources in the basin.

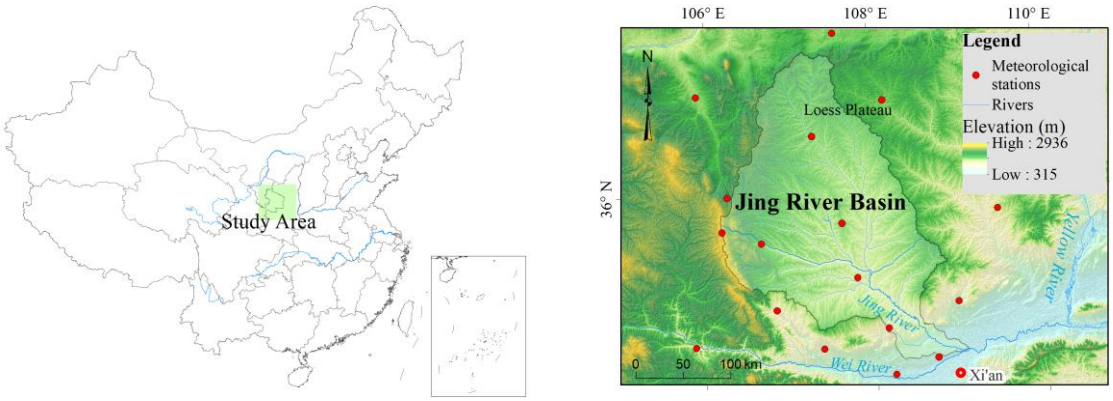

Fig. 1. Location map of the study area

2.2 Data

2.2.1 Climate

The daily meteorological data of the Jing River Basin from 1981 to 2020 were collected. Totally 18 meteorological stations' data were acquired from the China Meteorological Data Service Center (CMDSC 2021). The distribution of the meteorological stations is shown in Fig. 1.

2.2.2 NDVI

The MODIS product was chosen to analyze the spatial and temporal trends of NDVI. The Terra/MODIS Vegetation Indices Monthly L3 Global 1 km SIN Grid datasets were downloaded from the Level-1 and Atmosphere Archive & Distribution System (LAADS 2021) Distributed Active Archive Center (DAAC), located in the Goddard Space Flight Center in Greenbelt, Maryland (https://ladsweb.nascom.nasa.gov/). The data spatial resolution is 1000 m. The annual NDVI of the basin was generated by the Maximum Value Composite (MVC) method.

2.2.3 Land use and land cover

The land use and land cover data were acquired from the website of GlobeLand30 (Jun et al. 2014) (http://www.globallandcover.com/). The GlobeLand30 is a is 30-meter spatial resolution global land cover data product, developed by the National Geomatics Center of China (NGCC 2021) and supervised by the

136 Ministry of Natural Resources of the People's Republic of China.

137 *2.2.4 Digital elevation model (DEM)*

138 The elevation data were obtained from the website of the Consultative Group for International
139 Agricultural Research (CGIAR 2021). The data is measured by the Shuttle Radar Topographic Mission
140 (SRTM) project and produced by NASA. The spatial resolution of the DEM is 3 arc-second (about 90 m).

141 ## 3. Methods

142 *3.1. Getis-Ord Gi* statistic*

143 Among GIS tools, the Getis-Ord Gi* statistic is widely used for hot spot analysis. By calculating the Gi*
144 statistics of spatial features (spatial variable), it is possible to reflect the aggregation degree of the high value
145 area (hot spot) and low value area (cold spot) of the spatial variable (Chambers 2020, ESRI 2021). The
146 calculation is as follows (Getis and Ord 1992, Ord and Getis 1995):

147 $$G_i^* = \frac{\sum_{j=1}^{n} \omega_{i,j} x_j - \bar{X} \sum_{j=1}^{n} \omega_{i,j}}{S \sqrt{\frac{\left[n \sum_{j=1}^{n} \omega_{i,j}^2 - (\sum_{j=1}^{n} \omega_{i,j})^2 \right]}{n-1}}} \quad (1)$$

148 where x_j is the attribute value for spatial feature j, $\omega_{i,j}$ is the spatial weight between feature i and j, n
149 is the total number of features, and(Getis and Ord 1992, Ord and Getis 1995):

150 $$\bar{X} = \frac{\sum_{j=1}^{n} x_j}{n} \quad (2)$$

151 $$S = \sqrt{\frac{\sum_{j=1}^{n} x_j^2}{n} - (\bar{X})^2} \quad (3)$$

152 When the analyzed data is a time series, emerging hotspot analysis can identify the changing trend of the
153 data (Betty et al. 2020, ESRI 2021). For example, it can find new, enhanced, reduced, and scattered hot and
154 cold spots. The emerging hotspot analysis can classify the hot spot as patterns listed in Table 1 which defined
155 by ArcGIS online help documentation (classifications of the cold spot are similar) (ESRI 2021):

Table 1

Emerging hot spot patterns and the definitions

Pattern	Definition
No Pattern Detected	Does not fall into any of the hot or cold spot patterns defined.
New Hot Spot	A location that is a statistically significant hot spot during the final time step and has never been a statistically significant hot spot before.
Consecutive Hot Spot	A location with an uninterrupted run of the statistically significant hot spot bins in the last time step interval. The location has never become a statistically significant hot spot before the final hot spot run and less than 90% of all bins are statistically significant hot spots.
Intensifying Hot Spot	A location that has been a statistically significant hot spot for 90% of the time-step intervals, including the last time step. In addition, the clustering intensity of high counts in each time step is increasing overall and the increase is statistically significant.
Persistent Hot Spot	A location that has been a statistically significant hot spot for 90% of the time-step intervals with no perceptible trend indicating an increase or decrease in the clustering intensity over time.
Diminishing Hot Spot	A location that has been a statistically significant hot spot for 90% of the time-step intervals, including the last time step. In addition, the clustering intensity in each time step is generally decreasing and the decrease is statistically significant.
Sporadic Hot Spot	A location that is an on-again then off-again hot spot. Less than 90% of the time-step intervals have been statistically significant hot spots and no time-step intervals have been statistically significant cold spots.
Oscillating Hot Spot	A statistically significant hot spot for the last time-step interval that has a history of also being a statistically significant cold spot during a prior time step. Less than 90% of the time-step intervals have been statistically significant hot spots.
Historical Hot Spot	The most recent time period is not a hot spot, but at least 90% of the time-step intervals have been statistically significant hot spots.

In this study, the Getis-Ord Gi* statistic and the emerging hot spot analysis were implemented by Python and ArcGIS. In the analysis parameter setting, the time step interval is one year, space-time bin size is 1 km, and the neighborhood distance interval is 20 km.

3.2. Mann–Kendall trend test

The Mann–Kendall (Mann 1945) trend test method is widely used in many fields of geoscience. It uses the data sequence order to judge the correlation degree between two variables and achieve the variation trend of the long-term data series. The Mann-Kendall trend test statistic can be calculated as follows (Mann 1945):

$$S = \sum_{k=1}^{n-1} \sum_{j=k+1}^{n} \mathrm{sgn}(x_j - x_k) \tag{4}$$

where n is the length of the time series, x_j and x_k are the variable values in the time series ($j > k$). "sgn" is a symbolic function, and (Mann 1945):

$$\mathrm{sgn}(x_j - x_k) = \begin{cases} 1, & x_j - x_k > 0 \\ 0, & x_j - x_k = 0 \\ -1, & x_j - x_k < 0 \end{cases} \tag{5}$$

The Mann-Kendall trend test uses a significance level of trend (Z), and the slope of the trend (S) to determine the trend significance of data changes. The significance level indicates whether the trend is statistically significant, while the slope shows the degree and direction of the trend. The statistic Z can be calculated as follows (Mann 1945):

$$Z = \begin{cases} \dfrac{S-1}{\sqrt{VAR(S)}} & S > 0 \\ 0 & S = 0 \\ \dfrac{S+1}{\sqrt{VAR(S)}} & S < 0 \end{cases} \tag{6}$$

If $Z > 0$, the time series shows a monodic upward trend. If $Z < 0$, the time series shows a monodic downward trend. The absolute critical value of Z for the significance level 0.01, 0.05 and 0.1 are 2.576, 1.96 and 1.645, respectively.

The variance (S) can be calculated by the following equation (Mann 1945):

$$VAR(S) = \frac{1}{18}\left[n(n-1)(2n+5)\right] - \sum_{p=1}^{q} t_p(t_p-1)(2t_p+5) \tag{7}$$

where, q is the number of sets with the same variable value, t_p refers to data's number in the p_{th} set.

3.3. Pearson Correlation Coefficient

The Pearson correlation coefficient is used to measure the strength of a linear association between two variables, the equation is as follows (Forthofer et al. 2007):

$$r = \frac{\sum_{i=1}^{n}(x_i - \bar{x})(y_i - \bar{y})}{\sqrt{\sum_{i=1}^{n}(x_i - \bar{x})^2}\sqrt{\sum_{i=1}^{n}(y_i - \bar{y})^2}} \tag{8}$$

where r represents the Pearson correlation coefficient, x_i denotes the value of the variables x, and y_i is the value of the variable y, $\bar{x}$ refers to the arithmetic mean of variables x, and $\bar{y}$ is the arithmetic mean of variables y. The larger the absolute value of r, the stronger the correlation. When $r>0$, it indicates that the two variables are positively correlated, $r=1$ means a perfect positive correlation. When $r<0$, it indicates that the two variables are negatively correlated, and the value $r=-1$ means a perfect negative correlation. When $r=0$, it indicates that the two variables are not linearly related.

4. Results and discussion

4.1. Spatial trend of NDVI

The mean and coefficient of variation (CV) of the NDVI series in the Jing River Basin were generated by calculating the arithmetic mean of each cell in the time series of NDVI image, and the spatial distribution characteristics of the NDVI statistics in the basin are shown in Fig. 2.

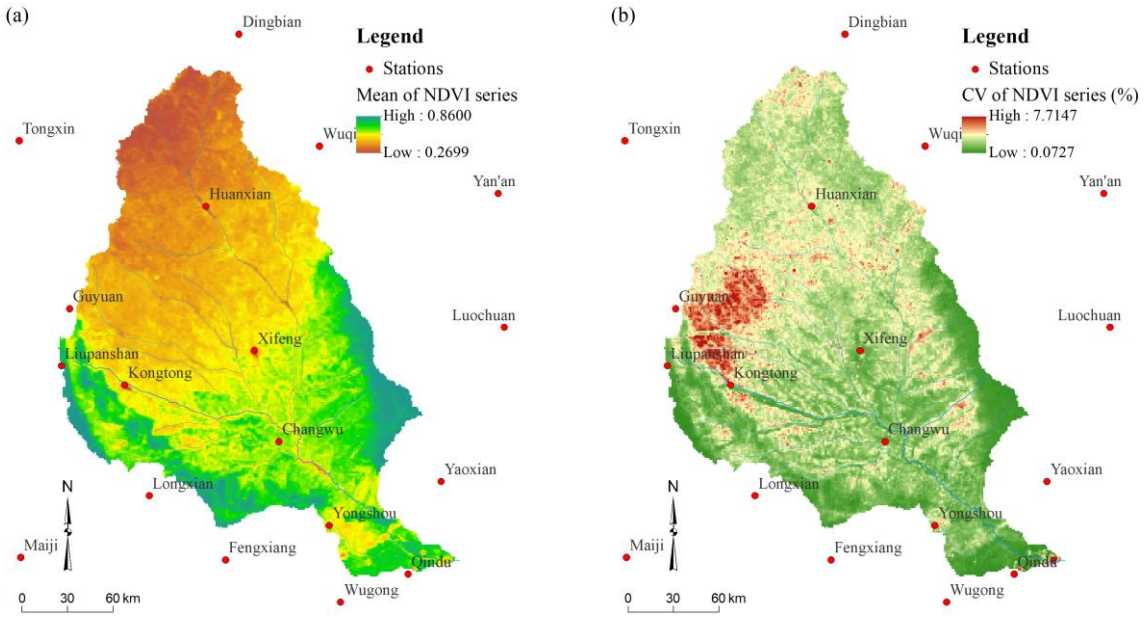

Fig. 2. Spatial distribution of NDVI statistics in the Jing River Basin, (a) Mean of NDVI, (b) CV of NDVI

The mean NDVI varies from 0.2699 to 0.8600 with an average of 0.5610, and shows a decreasing trend from southeast to northwest. The two wings of the basin had the highest value of NDVI. The NDVI in the north loess hilly region is the lowest. Zone of NDVI lower than 0.5610 mainly distributed in the upstream part divided by Guyuan, Kongtong, Xifeng, and Wuqi, which accounts for about 51.67% of the total area of the basin.

The CV of NDVI varies from 0.0727 % to 7.7147 % (average: 1.2776 %), shows an increasing trend from southeast to northwest which differs from the distribution of Mean NDVI. As can be seen from Fig.2 (b), there is a local aggregation of the high value of CV at the west of basin nearby Guyuan and Kongtong, indicating the vegetation coverage there varies stronger than other places in the basin.

4.2. Inter-annual variation characteristics of basin mean NDVI

The inter-annual variation of the NDVI in the Jing River Basin from 1998 to 2018 is shown in Fig. 3. The mean NDVI in the basin is 0.561, the minimum NDVI is 0.128 (2000), the maximum NDVI is 0.92 (2012). The NDVI anomaly changes from negative to positive in 2010, the overall NDVI shows an upward linear trend with the R^2 coefficient of 0.8363, indicating that the vegetation coverage changes better gradually in these two decades in Jing River Basin.

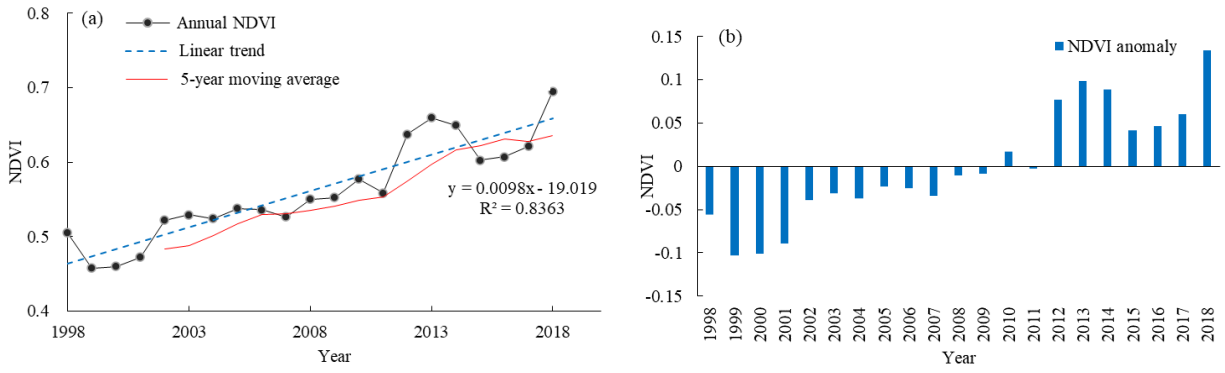

Fig. 3. The change curve of NDVI in the Jing River Basin, (a) annual NDVI and trend, (b) NDVI anomaly

4.3. Spatial patterns of NDVI emerging hot spots

Emerging hot spot analysis can reflect the aggregation pattern and trend of vegetation coverage, low NDVI value aggregating as the cold spot of vegetation coverage, while high NDVI value aggregating as the hot spot of vegetation coverage. During a period, the hot spot or cold spot emerges or diminishes with the variation of vegetation coverage. Using the emerging hot spot analysis tool analyzed the time series of NDVI data, the spatial patterns of emerging hot spots of NDVI are depicted in Fig.4. The NDVI statistics of each hot spot pattern and cold spot pattern are shown in Table 2.

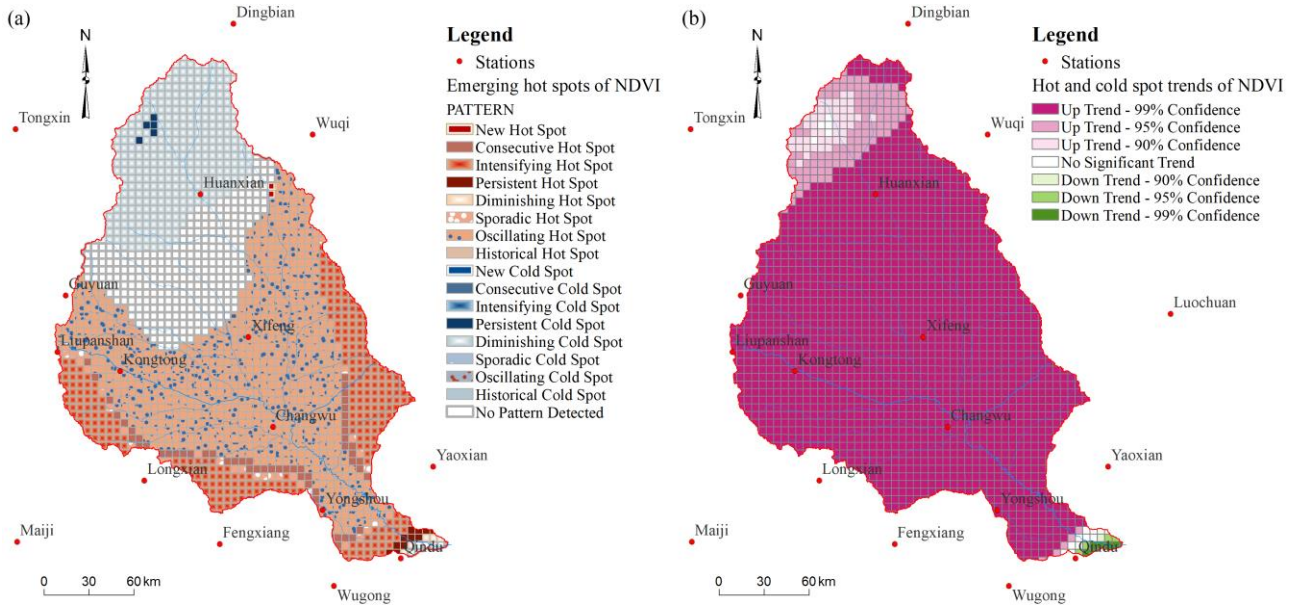

Fig. 4. Emerging hot spot patterns of NDVI in the Jing River Basin, (a) hot spot patterns, (b)hot spot trends

Table 2

The NDVI statistics of hot spot pattern and cold spot pattern in the Jing River Basin

Pattern	NDVI			
	MIN	MAX	Mean	STD
New Hot Spot	0.3539	0.6485	0.5026	0.0800
Consecutive Hot Spot	0.5262	0.7901	0.6664	0.0777
Intensifying Hot Spot	0.6507	0.8493	0.7562	0.0580
Persistent Hot Spot	0.6464	0.7855	0.7155	0.0357
Diminishing Hot Spot	0.5864	0.7771	0.6910	0.0496
Sporadic Hot Spot	0.5478	0.7879	0.6748	0.0695
Oscillating Hot Spot	0.4436	0.7270	0.5887	0.0800
Persistent Cold Spot	0.2206	0.4766	0.3187	0.0634
Diminishing Cold Spot	0.2509	0.5525	0.3822	0.0719
No Pattern Detected	0.3463	0.6556	0.4805	0.0863

At the upstream of the basin, the primary spatial pattern is diminishing cold spot, indicating that this region has been a statistically significant cold spot of vegetation coverage for more than 18 years during the whole period, including the year 2018. The intensity of clustering low vegetation coverage in each year is decreasing overall and the decrease is statistically significant. This region accounts for 18.41% of the total area of the basin. In addition, 2 small persistent cold spots are observed, which have been the statistically significant low value aggregation of vegetation coverage for 18 years with no discernible trend showing

increase or decrease in the clustering intensity of vegetation coverage over time.

In the mid-upstream of the basin, there is a strip between Huanxian and Xifeng that shows no obvious pattern of hot or cold spot, indicating that in this region no obvious aggregation pattern or trends of vegetation coverage was observed in these two decades. This strip accounts for 16.36 % of the total area of the basin.

At the central part of the mid-downstream of the basin, from Xifeng to Qindu, large scope of oscillating hot spot is observed, representing the vegetation coverage at this region is high in 2018, but also has a history of low coverage during a prior period, and the period of high vegetation coverage is less than 18 years during the last two decades. This pattern of vegetation coverage trend reaches 44.70 % of the total area of the basin.

The intensifying hot spot main distributes at the west wing and east wing of the basin, indicating that the vegetation coverage in these regions keeps high for more than 18 years during the period including the year 2018, and has a significant increasing trend in each year. The percentage of this pattern in the basin is 14.57%.

In addition, the proportions of the consecutive hot spot, the sporadic hot spot, the persistent hot spot, the diminishing hot spot, and the new hot spot in the basin are 3.00 %, 1.87 %, 0.47 %, 0.27 %, 0.22 %, and 0.11 %, respectively. The new cold spot, the consecutive cold spot, the intensifying cold spot, the sporadic cold spot, the oscillating cold spot, and the historical cold spot are not observed in the basin. The highest mean NDVI is observed in the intensifying hot spot region, while the lowest mean NDVI is observed in the persistent cold spot.

From Fig. 4b, it can be seen that almost the whole basin shows the statistically significant upward trend of high-value aggregation of NDVI, indicating that no matter hot spots or cold spots, the vegetation coverage in these regions has increased in general during the period.

4.4. Temporal trend of NDVI

As presented in the foregoing, the NDVI in the basin has obvious spatial differences and temporal trends. The time-series data of the NDVI in the Jing River Basin from 1998 to 2018 are analyzed using the Mann-Kendall test. Fig.5 depicted the spatial distribution of NDVI changing trends and statistical significance.

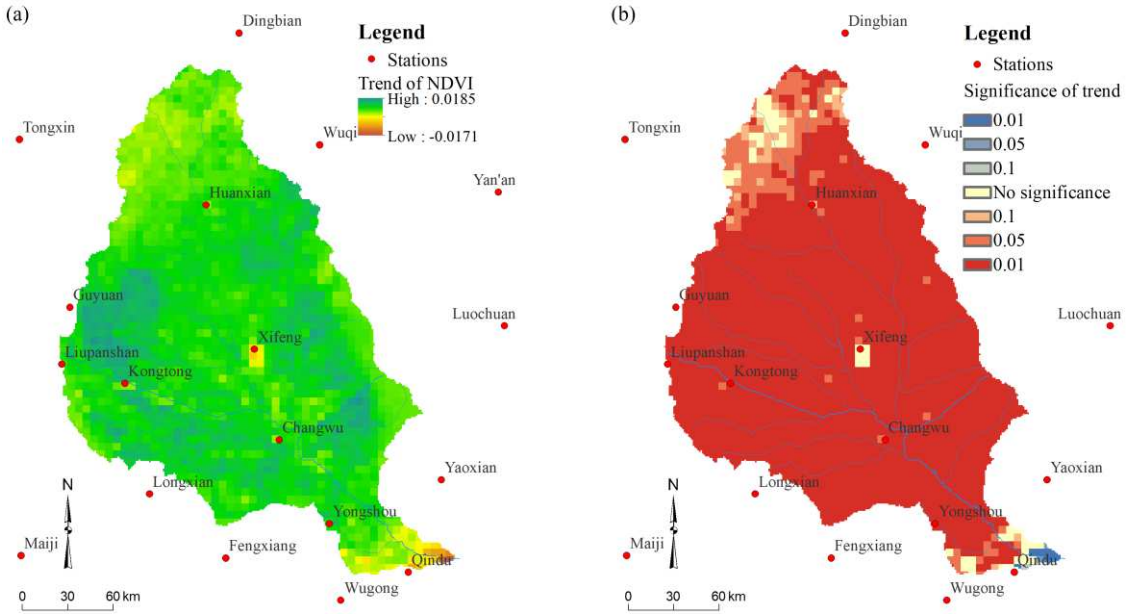

Fig. 5. Spatial distribution of the NDVI temporal trends. (a) trends of NDVI, (b) significance of trends

As shown in Fig. 5a, the variation rate of NDVI in the Jing River Basin varies from -0.0171 to 0.0185 per year, the average variation rate is 0.0095 per year. There is no obvious spatial trend of variation rate shown in the basin. However, the distributions of high variation rate are in consistent with the distributions of high CV of NDVI. The largest increase is found at Guyuan and Kongtong, and the decreasing trend is found at Qindu.

As can be seen from Fig. 5b, the trend of NDVI shows the significance of $P < 0.05$ and $P < 0.01$ at most of the basin, indicating that the increasing trend of vegetation coverage is significant.

Table 3

The NDVI temporal trend statistics of hot spot pattern and cold spot pattern in the Jing River Basin

Pattern	MIN	MAX	Range	Mean	STD
New Hot Spot	0.0101	0.0117	0.0015	0.0110	0.0007
Consecutive Hot Spot	0.0007	0.0169	0.0162	0.0111	0.0029
Intensifying Hot Spot	-0.0015	0.0185	0.0200	0.0085	0.0032
Persistent Hot Spot	-0.0053	0.0054	0.0107	0.0011	0.0028
Diminishing Hot Spot	-0.0095	0.0023	0.0118	-0.0046	0.0041
Sporadic Hot Spot	0.0007	0.0143	0.0137	0.0097	0.0027
Oscillating Hot Spot	-0.0024	0.0184	0.0208	0.0108	0.0026
Persistent Cold Spot	0.0029	0.0053	0.0024	0.0042	0.0006
Diminishing Cold Spot	0.0017	0.0115	0.0098	0.0066	0.0019
No Pattern Detected	-0.0171	0.0171	0.0342	0.0103	0.0031

The NDVI temporal trend statistics of each hot spot pattern and cold spot pattern are shown in Table 3. Among all patterns in the basin, only the diminishing hot spot has a negative mean trend of -0.0046, however,

it just accounts for 0.22 % of the basin and will not impact the general increasing trend of the vegetation coverage. The government may need to pay more attention to the oscillating hot spot region and the no pattern detected region. These two regions area covers more than 60 % of the basin. In these two regions, the downward trend may stronger or weaker than the upward trend alternately, implying that the environment may unstable and would evolve in an uncertain direction.

4.5. Relationships between NDVI and climate, anthropological activities

According to previous similar studies results, the NDVI mainly affected by climate and anthropological activities (Zhang et al. 2018b, Jin et al. 2021). The relationship between the NDVI time series and the precipitation time series was analyzed using the Pearson correlation coefficient.

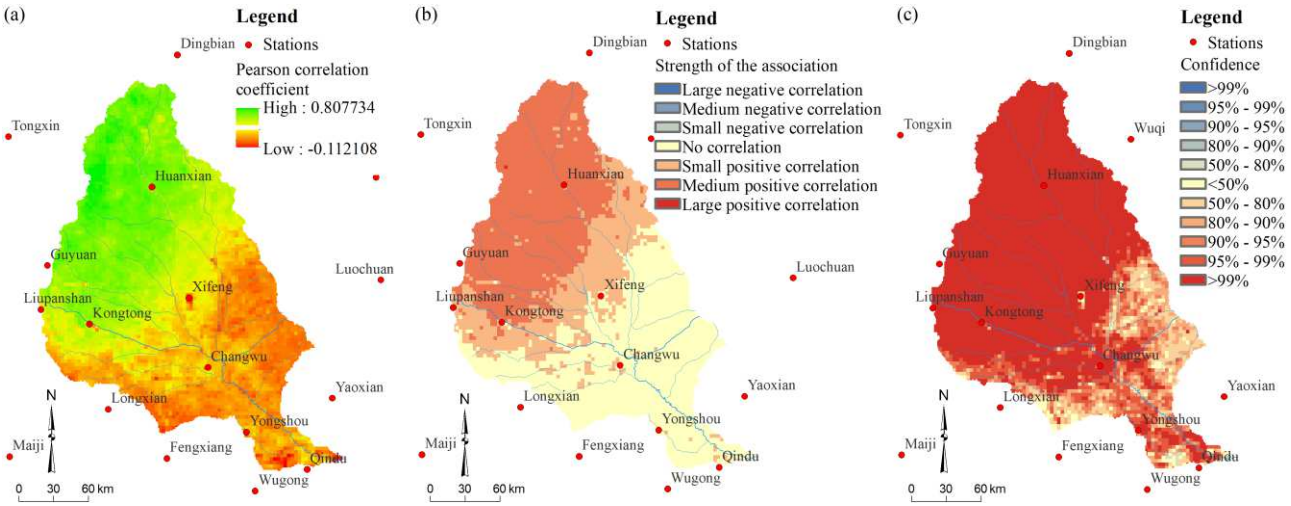

Fig. 6. Spatial distribution of Pearson correlation analysis results in the Jing River Basin, (a) Pearson correlation coefficient, (b) strength of the association, (c) statistical confidence

As shown in Fig.6, the Pearson correlation coefficient varies from -0.1121 to 0.8077 with an average of 0.3863. The positive correlation mainly observed upstream of the basin. In the Loess Plateau, the lower the NDVI, the larger the correlation between NDVI and precipitation is, revealing that the growth of vegetation in this region is more dependent on the water supply from the precipitation. At the mid and downstream of the basin, the strength of the association is weak, showing that climate change may have limited impacts on the vegetation coverage there during the period. The statistical confidence data signify that the correlation analysis results are statistically significant at the mid and upstream basin but uncertain at part of the downstream basin.

Land use and land cover change are the predominant anthropological activities that will change the

vegetation coverage. Cultivated land, forest, grassland, and shrub are four major land cover that can reflect the regional vegetation coverage. Fig. 7 demonstrates the four major land cover transition happened in the basin from 2000 to 2020. The statistics of land cover transition are shown in Table 4.

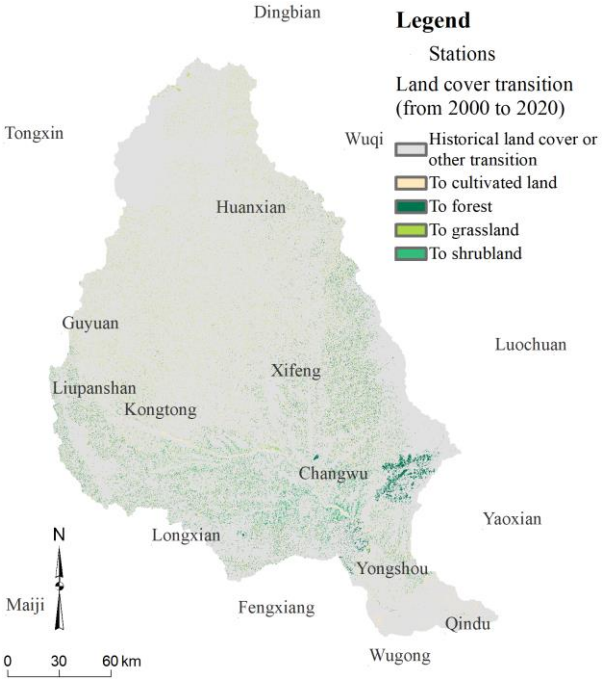

Fig. 7. Land cover transition happened in the Jing River Basin from 2000 to 2020

Table 4

Land cover transition statistics of the Jing River Basin

Category in 2000	Category proportion (%)					Total in 2000
	Cultivated land	Forest	Grassland	Shrubland	Other	
Cultivated land	43.68	0.51	2.29	0.07	1.50	48.05
Forest	0.36	14.23	1.28	0.15	0.02	16.04
Grassland	2.54	1.65	29.12	0.35	0.12	33.77
Shrubland	0.02	0.10	0.15	0.46	0.00	0.73
Other	0.42	0.01	0.06	0.00	0.91	1.40
Total in 2020	47.01	16.50	32.90	1.04	2.55	100.00

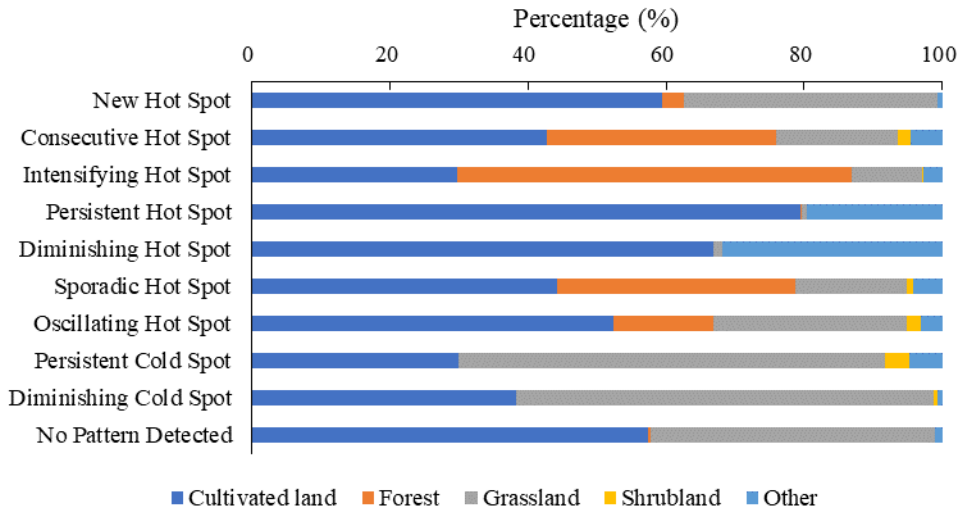

Fig. 8. Land cover proportions of hot spot patterns in the Jing River Basin

As can be seen in Fig. 7, forest and shrubland mainly transited at the downstream of the basin, cultivated mainly transited at the upstream of the basin, while grassland mainly transited at the mid and the upstream of the basin. During the period of 2000 to 2020, forest and shrubland has increased 0.46 % and 0.31 %, respectively. Cultivated land and grassland has decreased 1.04 % and 0.87 %, respectively. As shown in Fig. 8, the primary mixed land cover patterns in diminishing hot spot, no pattern detected region, oscillating hot spot, intensifying hot spot are grassland-cultivated land, cultivated land-grassland, cultivated land-grassland-forest, forest-cultivated land-grassland, respectively. These transition patterns and the primary mixed land cover patterns can explain the spatiotemporal trend of NDVI analyzed foregoing.

On the views above, the change characteristics and evolving path of NDVI in the Jing River Basin are clear and obvious. According to the previous studies, the vegetation change has improved the soil and water conservation situation. Moreover, the increased vegetation, especially the forest has a positive effect on promoting the capacity of carbon sequestration and oxygen release (Paustian 2014). However, it has also impacted the runoff of the Jing River and cause water utilization conflict in agricultural development (Zhang et al. 2021). The increased vegetation also consumes more water than ever and arise the problem of loss of soil moisture and the depletion of groundwater, the formed vicious circle feedback limits the vegetation growth. Therefore, it is better for the government to strengthen the monitor of the environment and the ecosystem from a global view, balance the relationship between social development the natural resource management, ensure the achievement of sustainable development goals.

5. Conclusions

In the present study, the NDVI, precipitation data of the Jing River Basin were collected, the emerging hot spot and cold spot patterns of NDVI were examined, the temporal trends, spatial distributions and changing patterns of the NDVI in the basin have been analyzed, the impacts on NDVI changes from climate, land cover change have been discussed. The conclusions can be summarized:

(1) The spatial distribution characteristics of NDVI indicate that the NDVI in Jing River Basin shows a spatial trend of decreasing from northwest to southeast. The two wings of the basin had the highest value of NDVI. The NDVI in the north loess hilly region is the lowest.

(2) The emerging hot spot analysis results show that diminishing cold spot, oscillating hot spot, intensifying hot spot are predominant patterns in the basin. The region of no pattern detected also covers a large area of the mid and upstream. The whole basin shows the statistically significant upward trend of high-value aggregation of NDVI, indicating that no matter hot spots or cold spots, the vegetation coverage in these regions has increased overall during the period.

(3) The temporal trend of NDVI in the basin varies from-0.0171 to 0.0185 per year, the average variation rate is 0.0095 per year. No obvious spatial trend of variation rate was observed in the basin. The increasing trend of vegetation coverage in the basin is statistically significant.

(4) The positive correlation between the NDVI and the precipitation mainly observed upstream of the basin. In the Loess Plateau, the lower the NDVI, the larger the correlation between NDVI and precipitation is, revealing that the growth of vegetation in this region is more dependent on the water supply from the precipitation. At the mid and downstream of the basin, the strength of the association is weak, showing that climate change may have limited impacts on the vegetation coverage there during the period.

(5) Anthropological activities have been changing the land cover patterns in the Jing River Basin. During the period of 2000 to 2020, forest and shrubland has increased 0.46 % and 0.31 %, respectively. Cultivated land and grassland has decreased 1.04 % and 0.87 %, respectively. Land cover transition patterns and the land cover patterns also impact the spatial and temporal trends of the vegetation coverage in the basin.

Acknowledgements

This research was supported by the National Natural Science Foundation of China (41971033), the Natural Science Basic Research in Shaanxi Province of China (Program No. 2019JM-512), the Key

Laboratory of Degraded and Unused Land Consolidation Engineering of the Ministry of Natural Resources (SXDJ2019-13), the Fundamental Research Funds for the Central Universities (CHD300102291507), the Programme of Introducing Talents of Discipline to Universities (B08039), Fund Project of Shaanxi Key Laboratory of Land Consolidation (2019-JC01).

References

Aber JS, Marzolff I, Ries JB (2010) Chapter 16 - Vegetation and Erosion. In: Aber JS, Marzolff I, Ries JB (eds) Small-Format Aerial Photography. Elsevier, Amsterdam, pp 219–228

Betty EL, Bollard B, Murphy S, et al (2020) Using emerging hot spot analysis of stranding records to inform conservation management of a data-poor cetacean species. Biodivers Conserv 29:643–665. https://doi.org/10.1007/s10531-019-01903-8

CGIAR CG for IAR CGIAR-CSI SRTM – SRTM 90m DEM Digital Elevation Database. https://srtm.csi.cgiar.org/. Accessed 12 Apr 2021

China Meteorological Data Service Center, 2019. Dataset of daily climate data from Chinese surface stations for global exchange (V3.0). http://data.cma.cn/en. Accessed 10 March. 2021.

Chambers SN (2020) The spatiotemporal forming of a state of exception: repurposing hot-spot analysis to map bare-life in Southern Arizona's borderlands. GeoJournal 85:1373–1384. https://doi.org/10.1007/s10708-019-10027-z

Chang J, Li Y, Wei J, et al (2016) Dynamic changes of sediment load and water discharge in the Weihe River, China. Environ Earth Sci 75:1042. https://doi.org/10.1007/s12665-016-5841-9

Delang CO, Yuan Z (2015) Ecological and Environmental Impact. In: Delang CO, Yuan Z (eds) China's Grain for Green Program: A Review of the Largest Ecological Restoration and Rural Development Program in the World. Springer International Publishing, Cham, pp 135–145

Deng L, Xu B, Yang X, Hu A (2021) Water quality and health risk assessment based on hydrochemical characteristics of tap and large-size bottled water from the main cities and towns in Guanzhong Basin, China. Environ Earth Sci 80:139. https://doi.org/10.1007/s12665-021-09415-x

ESRI Emerging Hot Spot Analysis—Help | ArcGIS for Desktop. https://desktop.arcgis.com/en/arcmap/10.3/tools/space-time-pattern-mining-toolbox/emerginghotspots.htm. Accessed 11 Apr 2021

Forthofer RN, Lee ES, Hernandez M (2007) 13 - Linear Regression. In: Forthofer RN, Lee ES, Hernandez M (eds) Biostatistics (Second Edition). Academic Press, San Diego, pp 349–386

Getis A, Ord JK (1992) The Analysis of Spatial Association by Use of Distance Statistics. Geographical Analysis 24:189–206. https://doi.org/10.1111/j.1538-4632.1992.tb00261.x

He S, Wu J (2019) Relationships of groundwater quality and associated health risks with land use/land cover patterns: a

384 case study in a loess area, northwest China. Hum Ecol Risk Assess 25(1-2):354-373.
385 https://doi.org/10.1080/10807039.2019.1570463

386 He S, Li P, Wu J, Elumalai V, Adimalla N (2020) Groundwater quality under land use/land cover changes: A temporal
387 study from 2005 to 2015 in Xi'an, northwest China. Hum Ecol Risk Assess 26(10):2771-2797.
388 https://dx.doi.org/10.1080/10807039.2019.1684186

389 Huang S, Tang L, Hupy JP, et al (2021) A commentary review on the use of normalized difference vegetation index
390 (NDVI) in the era of popular remote sensing. J For Res 32:1–6. https://doi.org/10.1007/s11676-020-01155-1

391 Jin F, Yang W, Fu J, Li Z (2021) Effects of vegetation and climate on the changes of soil erosion in the Loess Plateau of
392 China. Science of The Total Environment 773:145514. https://doi.org/10.1016/j.scitotenv.2021.145514

393 Jun C, Ban Y, Li S (2014) Open access to Earth land-cover map. Nature 514:434–434. https://doi.org/10.1038/514434c

394 Kriegler FJ, Malila WA, Nalepka RF, Richardson WD (1969) Preprocessing Transformations and Their Effects on
395 Multispectral Recognition. In Proceedings of the 6th International Symposium on Remote Sensing of
396 Environment, Ann Arbor, MI, USA, 13–16 October 1969; pp. 97–131.

397 LAADS Level-1 and Atmosphere Archive & Distribution System. https://ladsweb.modaps.eosdis.nasa.gov/. Accessed
398 12 Apr 2021

399 Li P (2020a) Meeting the environmental challenges. Hum Ecol Risk Assess 26(9):2303-2315.
400 https://doi.org/10.1080/10807039.2020.1797472

401 Li P (2020b) To make the water safer. Expo Health 12(3):337-342. https://doi.org/10.1007/s12403-020-00370-9

402 Li Z, Liu W, Zheng F (2013) The land use changes and its relationship with topographic factors in the Jing river
403 catchment on the Loess Plateau of China. SpringerPlus 2:S3. https://doi.org/10.1186/2193-1801-2-S1-S3

404 Li P, Qian H, Wu J, Chen J, Zhang Y, Zhang H (2014) Occurrence and hydrogeochemistry of fluoride in shallow
405 alluvial aquifer of Weihe River, China. Environ Earth Sci 71(7):3133-3145.
406 https://doi.org/10.1007/s12665-013-2691-6

407 Li P, He S, Yang N, Xiang G (2018) Groundwater quality assessment for domestic and agricultural purposes in Yan'an
408 City, northwest China: implications to sustainable groundwater quality management on the Loess Plateau.
409 Environ Earth Sci 77(23):775. https://doi.org/10.1007/s12665-018-7968-3

410 Li P, He X, Li Y, Xiang G (2019a) Occurrence and health implication of fluoride in groundwater of loess aquifer in the
411 Chinese Loess Plateau: a case study of Tongchuan, northwest China. Expo Health 11(2):95-107.
412 https://doi.org/10.1007/s12403-018-0278-x

413 Li P, He X, Guo W (2019b) Spatial groundwater quality and potential health risks due to nitrate ingestion through
414 drinking water: a case study in Yan'an City on the Loess Plateau of northwest China. Hum Ecol Risk Assess
415 25(1-2):11-31. https://doi.org/10.1080/10807039.2018.1553612

416 Liu S, Huang S, Xie Y, et al (2018) Spatial-temporal changes of rainfall erosivity in the loess plateau, China: Changing
417 patterns, causes and implications. CATENA 166:279–289. https://doi.org/10.1016/j.catena.2018.04.015

418 Mann HB, (1945) Nonparametric test against trend. Econometrica 13, 245–259. https://doi.org/10.2307/1907187

419 NGCC NGC of C GlobeLand30. http://www.globallandcover.com/home_en.html. Accessed 12 Apr 2021

420 Ning T, Li Z, Liu W (2016) Separating the impacts of climate change and land surface alteration on runoff reduction in
421 the Jing River catchment of China. CATENA 147:80–86. https://doi.org/10.1016/j.catena.2016.06.041

422 Ord JK, Getis A (1995) Local Spatial Autocorrelation Statistics: Distributional Issues and an Application. Geographical
423 Analysis 27:286–306. https://doi.org/10.1111/j.1538-4632.1995.tb00912.x

424 Paustian K (2014) Carbon Sequestration in Soil and Vegetation and Greenhouse Gases Emissions Reduction. In:
425 Freedman B (ed) Global Environmental Change. Springer Netherlands, Dordrecht, pp 399–406

426 Wang K, Deng L, Ren Z, et al (2016) Dynamics of ecosystem carbon stocks during vegetation restoration on the Loess
427 Plateau of China. J Arid Land 8:207–220. https://doi.org/10.1007/s40333-015-0091-3

428 Xu B, Zhang Y, Wang J (2019) Hydrogeochemistry and human health risks of groundwater fluoride in Jinhuiqu
429 irrigation district of Wei river basin, China. Hum Ecol Risk Assess 25(1-2):230–249.
430 https://doi.org/10.1080/10807039.2018.1530939

431 Zhang Y, Wu J, Xu B (2018a) Human health risk assessment of groundwater nitrogen pollution in Jinghui canal
432 irrigation area of the loess region, northwest China. Environ Earth Sci 77(7):273.
433 https://doi.org/10.1007/s12665-018-7456-9

434 Zhang H, Chang J, Zhang L, et al (2018b) NDVI dynamic changes and their relationship with meteorological factors
435 and soil moisture. Environ Earth Sci 77:582. https://doi.org/10.1007/s12665-018-7759-x

436 Zhang Y, Chao Y, Fan R, et al (2021) Spatial-temporal trends of rainfall erosivity and its implication for sustainable
437 agriculture in the Wei River Basin of China. Agricultural Water Management 245:106557.
438 https://doi.org/10.1016/j.agwat.2020.106557

439 Zhang Y, Xiong Y, Chao Y, et al (2020) Hydrogeochemistry and quality assessment of groundwater in Jinghui canal
440 irrigation district of China. Hum Ecol Risk Assess 26:2349–2366.
441 https://doi.org/10.1080/10807039.2020.1774737

442 Zhang Z, Huang M (2021) Effect of root-zone vertical soil moisture heterogeneity on water transport safety in
443 soil-plant-atmosphere continuum in Robinia pseudoacacia. Agricultural Water Management 246:106702.
444 https://doi.org/10.1016/j.agwat.2020.106702

Figures

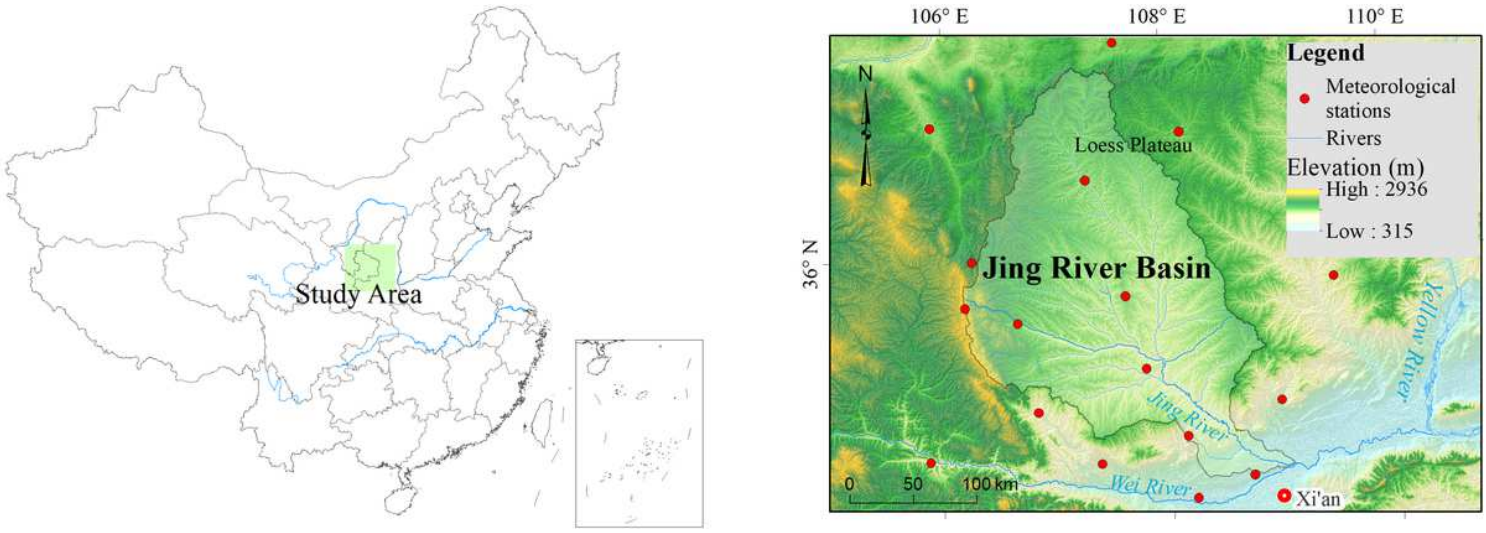

Figure 1

Location map of the study area Note: The designations employed and the presentation of the material on this map do not imply the expression of any opinion whatsoever on the part of Research Square concerning the legal status of any country, territory, city or area or of its authorities, or concerning the delimitation of its frontiers or boundaries. This map has been provided by the authors.

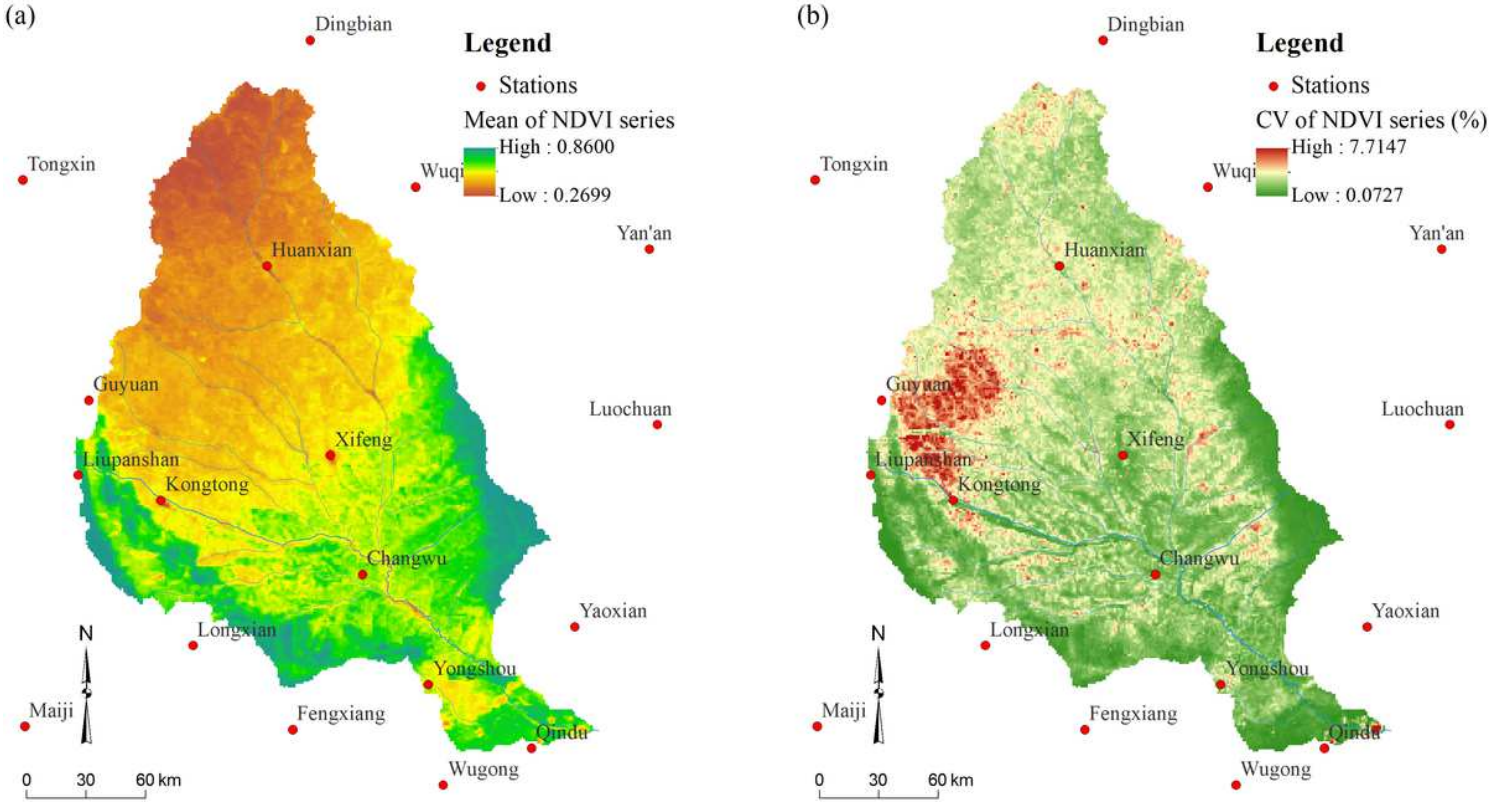

Figure 2

Spatial distribution of NDVI statistics in the Jing River Basin, (a) Mean of NDVI, (b) CV of NDVI Note: The designations employed and the presentation of the material on this map do not imply the expression of any opinion whatsoever on the part of Research Square concerning the legal status of any country, territory, city or area or of its authorities, or concerning the delimitation of its frontiers or boundaries. This map has been provided by the authors.

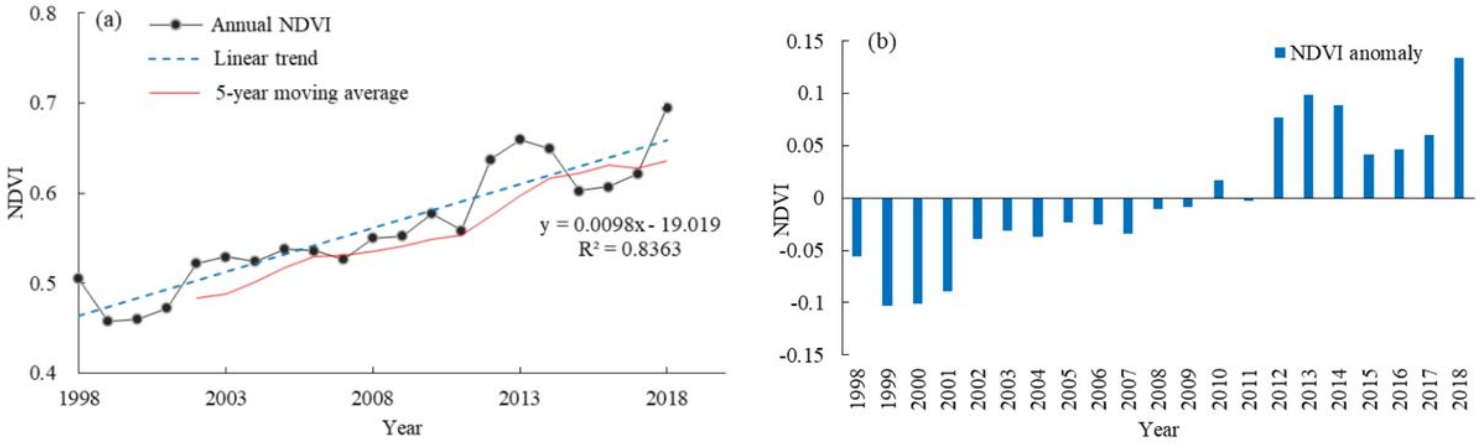

Figure 3

The change curve of NDVI in the Jing River Basin, (a) annual NDVI and trend, (b) NDVI anomaly

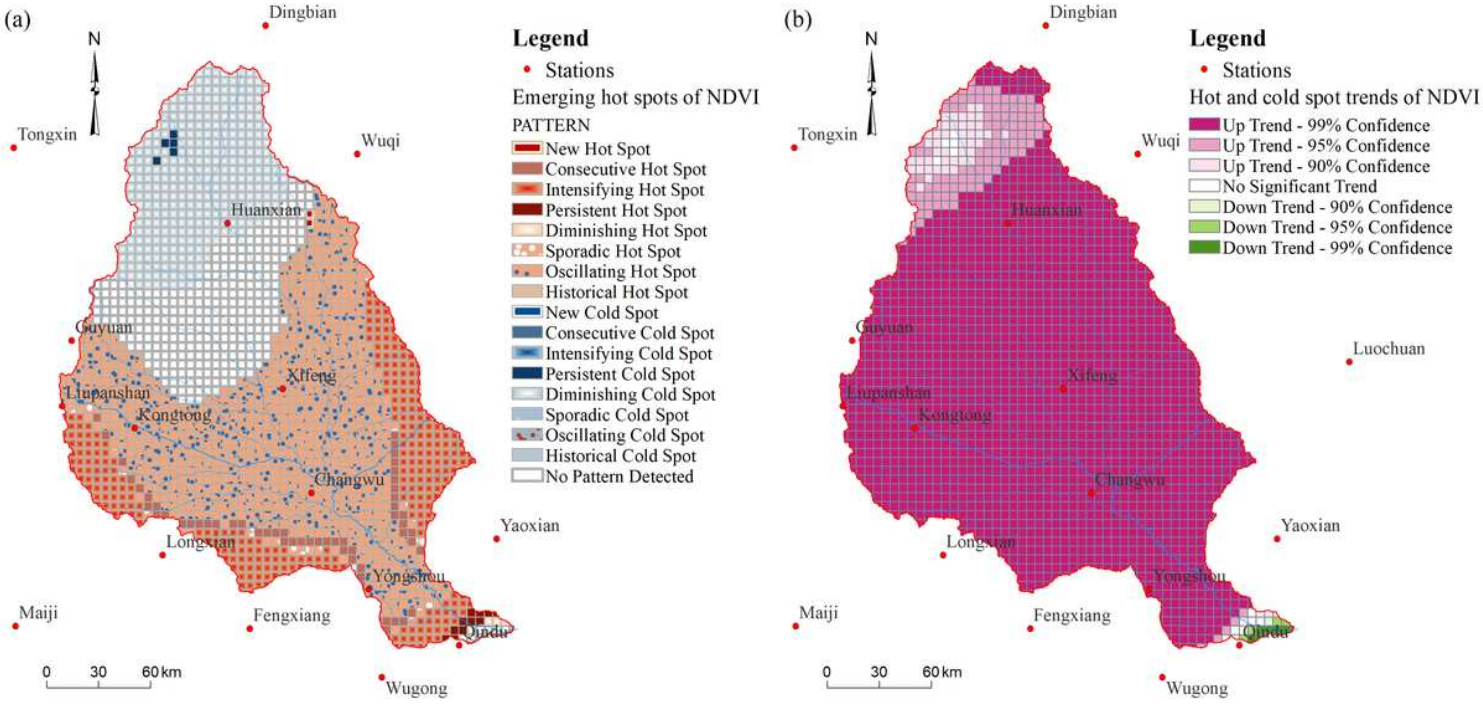

Figure 4

Emerging hot spot patterns of NDVI in the Jing River Basin, (a) hot spot patterns, (b)hot spot trends Note: The designations employed and the presentation of the material on this map do not imply the expression of any opinion whatsoever on the part of Research Square concerning the legal status of any country,

territory, city or area or of its authorities, or concerning the delimitation of its frontiers or boundaries. This map has been provided by the authors.

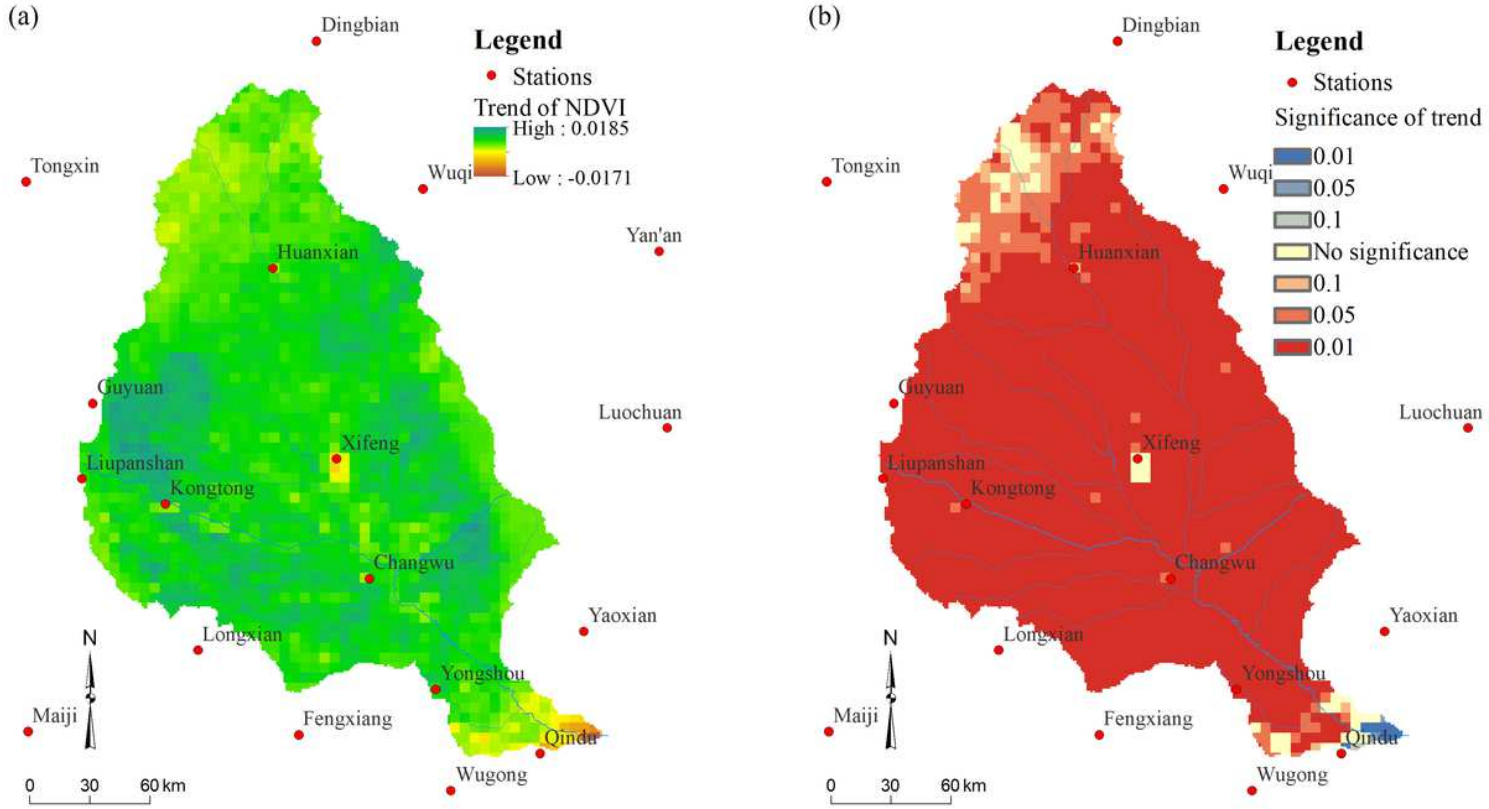

Figure 5

Spatial distribution of the NDVI temporal trends. (a) trends of NDVI, (b) significance of trends Note: The designations employed and the presentation of the material on this map do not imply the expression of any opinion whatsoever on the part of Research Square concerning the legal status of any country, territory, city or area or of its authorities, or concerning the delimitation of its frontiers or boundaries. This map has been provided by the authors.

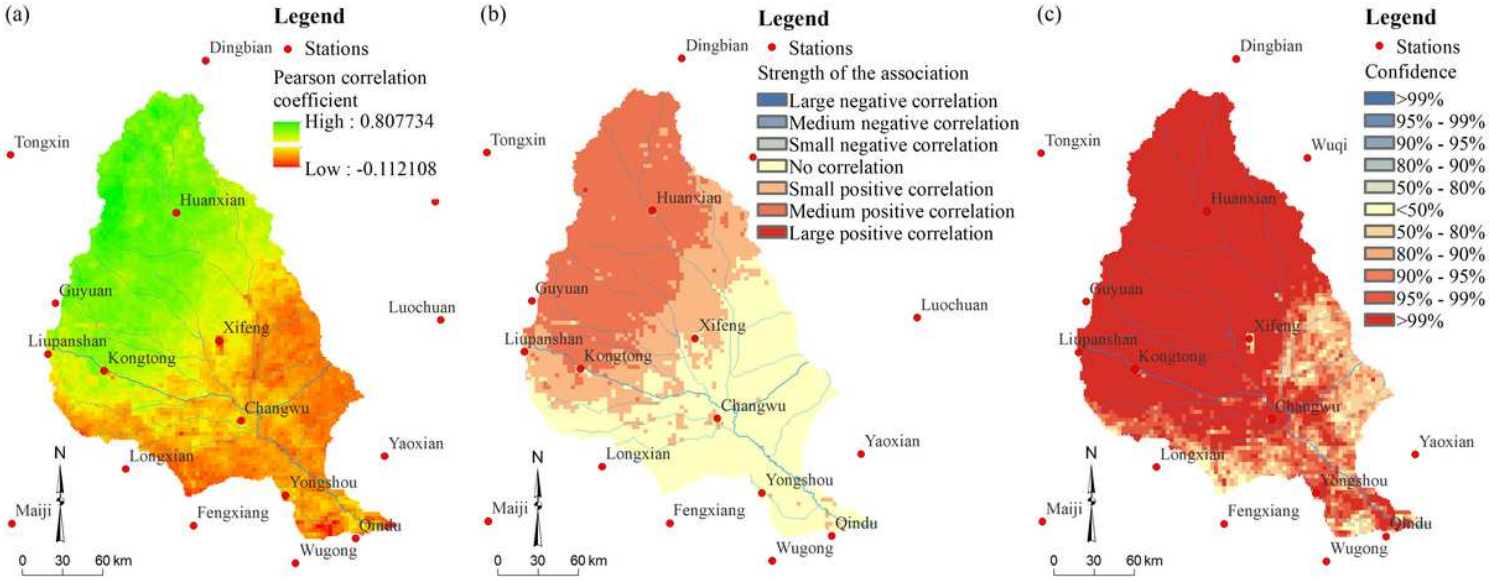

Figure 6

Spatial distribution of Pearson correlation analysis results in the Jing River Basin, (a) Pearson correlation coefficient, (b) strength of the association, (c) statistical confidence Note: The designations employed and the presentation of the material on this map do not imply the expression of any opinion whatsoever on the part of Research Square concerning the legal status of any country, territory, city or area or of its authorities, or concerning the delimitation of its frontiers or boundaries. This map has been provided by the authors.

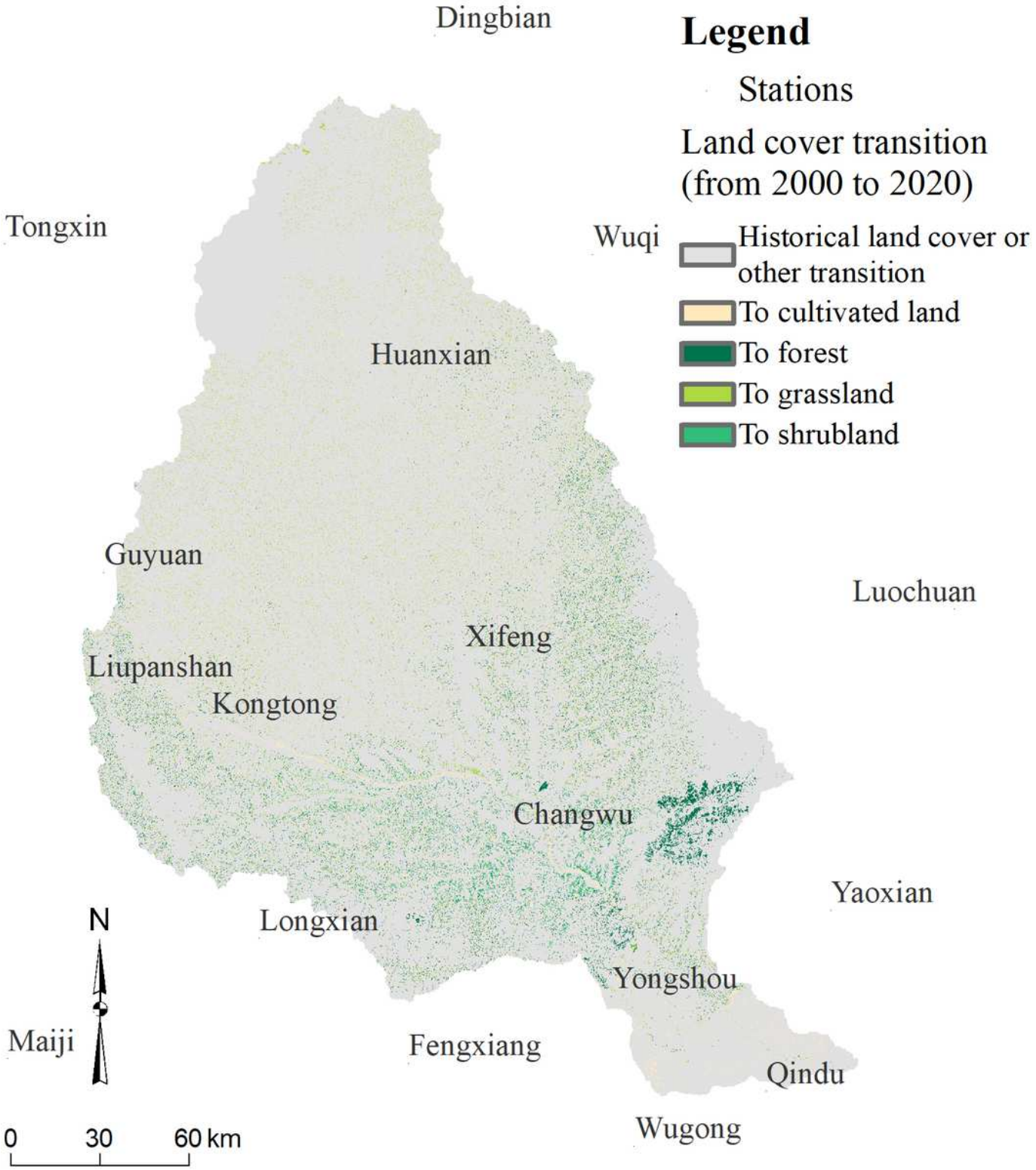

Figure 7

Land cover transition happened in the Jing River Basin from 2000 to 2020 Note: The designations employed and the presentation of the material on this map do not imply the expression of any opinion whatsoever on the part of Research Square concerning the legal status of any country, territory, city or area or of its authorities, or concerning the delimitation of its frontiers or boundaries. This map has been provided by the authors.

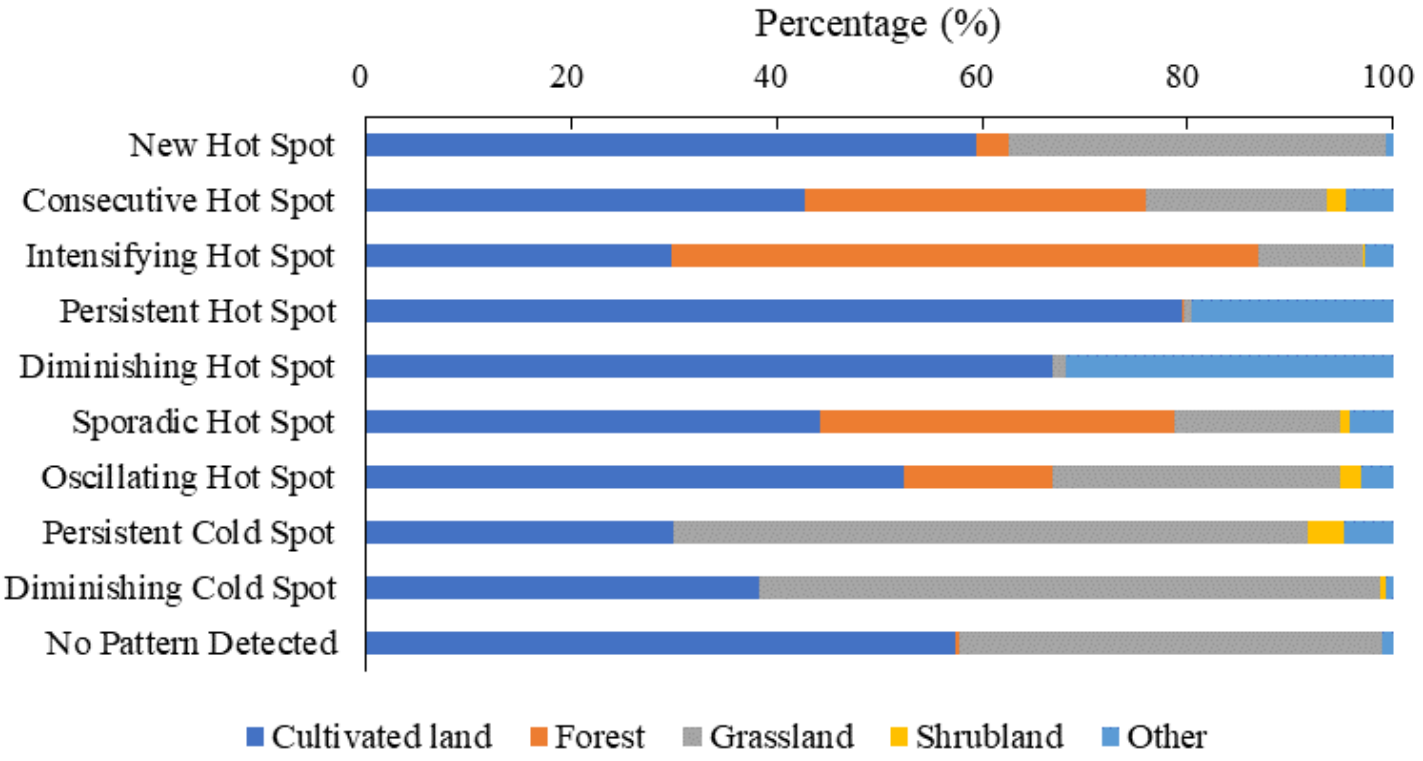

Figure 8

Land cover proportions of hot spot patterns in the Jing River Basin